

Development of Pd Supported Catalysts Using Thiol-Functionalized Mesoporous Silica Frameworks: Application to the Chemo- and Regioselective C-3 Arylation of Free-Indole

Marc Renom Carrasco,^[a] Walid Khodja,^[a] Clément Demarcy,^[a] Laurent Veyre,^[a] Clément Camp,^[a] and Chloé Thieuleux*^[a]

We report here the development of Pd-supported catalysts for the selective C-3 arylation of free-indole using thiol-functionalized silica supports to anchor the palladium centers. The palladium (II) complex, Pd(OAc)₂, was efficiently loaded into various thiol-functionalized mesostructured silicas at room temperature. These materials exhibit different contents of surface SH groups (0.3 to 1.8 SH/nm²) and various SH/Pd molar ratios from 6 to 65. It was found that the catalysts containing the most isolated surface SH groups (0.3 SH/nm²) and the highest loading of Pd were the most active, reaching 70% of conversion, 1400 as turnover numbers and 100% selectivity in

the C-3 arylated product using only 0.05 mol% of Pd. However, a leaching of active Pd species (1.7 ppm) was detected. The best compromise was found for a specific solid containing isolated surface thiol groups (0.3 SH/nm²) and a very low loading of Pd (SH/Pd = 65). It exhibited a high TON (608) with a very low Pd leaching of 0.5 ppm in the course of the catalytic reaction. These results thus illustrate that both surface SH sites isolation and concentration, as well as the SH/Pd molar ratio are key parameters to access high catalytic performances and very low leaching of metal during catalysis.

Introduction

Heterobiaryl compounds, among which aryl-indole derivatives, were identified in the last decade as promising synthons in active pharmaceutical ingredients to cure, for instance, diseases caused by microbial agents.^[1,2] They could also take part of potential treatments for non-microbial illnesses, such as diabetes, by acting directly on specific enzymes.^[3] Thus, elaborating new efficient chemical synthesis methods to yield these compounds is of the utmost interest.

To reach this goal, active molecular catalytic systems were therefore developed^[4–12] to address the challenging chemo- and regio-selective arylation of indoles at the C-3 position. The few reported systems, based on palladium or iridium metals, that were able to achieve this reaction with high selectivity toward the C-3 arylated product, exhibited moderate TONs of ca 80 at maximum.^[13–19] One exception is the catalytic system based on Pd(OAc)₂ and lithium bis(trimethylsilyl)amide that our group

recently reported and that was able to achieve this targeted reaction with a TON of 1800 and very high yield in C-3 product (90%).^[20] This reaction was also studied using transition metal free systems. Two salient examples are worth of note: i) the system reported by Chen *et al.*, using four equivalents of potassium *tert*-butoxide and an excess of indole, allowed to reach high yields (76% of the C-3 arylated product), albeit with low regioselectivity^[21] and ii) the system developed by Ackermann *et al.* which involved the use of substituted diaryliodonium salts as reagents, afforded the exclusive production of the C-3 arylated products, albeit with moderate yields.^[22] Overall, one can notice that most of the reported systems face two major problems: the lack of productivity and/or regioselectivity when using standard experimental conditions.

Moreover, the reported metal-based catalysts have a common drawback: the metal complexes or their deactivated forms (metallic particles) are not easy to separate from the reaction products and residual metal species are present in the products, even after several purification steps. This metallic pollution represents an issue, especially for the pharmaceutical industry, for which a threshold limit of palladium in drugs was set at 5–10 ppm by the European Agency for the Evaluation of Medicinal Products (EMA). To overcome this issue, heterogeneous catalysts could be of huge interest and preferred since they can be easily separated from the reaction mixture by a simple filtration step when used in batch reactors or without any purification step when used in continuous flow reactors.

Even though supported catalysis seems promising regarding purification considerations, palladium leaching during the catalytic reaction could occur. The use of scavenger materials to trap metal ions released from the catalyst during the reaction

[a] Dr. M. Renom Carrasco, Dr. W. Khodja, C. Demarcy, L. Veyre, Dr. C. Camp, Dr. C. Thieuleux
Institut de Chimie de Lyon,
Laboratory of Chemistry, Catalysis,
Polymers and Processes,
C2P2 UMR 5265 CNRS-UCB Lyon 1-CPE Lyon,
CPE Lyon,
Université de Lyon,
43 Bd du 11 Novembre 1918,
69616 Villeurbanne, France
E-mail: chloe.thieuleux@univ-lyon1.fr

Supporting information for this article is available on the WWW under <https://doi.org/10.1002/ejic.202001086>

Part of the "Supported Catalysts" Special Collection.

was reported.^[23] Most of these scavengers contain thiol groups, which strongly coordinate metal atoms. Indeed, several scavengers have been described for the entrapment of mercury,^[24] platinum,^[25] palladium,^[23,25] cadmium,^[26] zinc,^[27] silver^[28] and gold^[29,30] cations. In addition to their scavenging properties towards metals, these materials can be very efficient catalysts for various C–C cross coupling reactions, such as Heck-Mizoroki,^[31–34] Suzuki-Miyaura,^[31–37] Sonogashira^[36,38,39] reactions, olefin hydrogenation^[40] and thiophene derivatives arylation^[41] for instance. In this context, we envision here the development of thiol containing materials to strongly coordinate palladium atoms, as scavengers could do, but that would be able to catalyze efficiently the chemo- and regio-selective arylation of free-indole in C-3 position.

To achieve this goal, we prepared Pd-supported catalysts by coordination of Pd(OAc)₂ onto several mesostructured silica supports containing different densities of surface thiol groups and compared their catalytic performances to commercially available sulfur-containing polymeric supports (smopex®) classically used as scavengers. Our catalysts are based on specific mesostructured silica matrices that contain regularly distributed thiol groups at the surface of the pore channels with various thiol contents. All these solids were successfully metalated with Pd(OAc)₂ and used as catalysts for the selective C-3 arylation of free indole.

Results and Discussion

The silica matrices containing surface thiol groups were prepared by sol-gel process using a templating route. The materials were obtained *via* co-hydrolysis and co-condensation of (3-mercaptopropyl)triethoxysilane and tetraethyl orthosilicate (TEOS), in different molar ratios using Pluronic® P123 as the structure directing agent in acidic conditions (aqueous HCl solution, pH = 1.5), and the subsequent addition of NaF at 45 °C. The suspensions were further stirred for 72 h and the resulting solids were recovered by filtration. The P123 surfactant was then removed by Soxhlet extraction and the solids were collected, washed and dried at 135 °C under vacuum (Scheme 1-see experimental section for details).

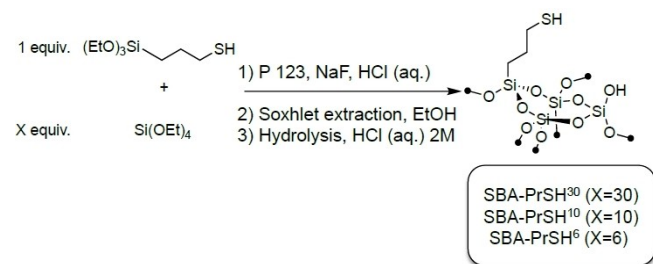
This synthetic protocol was chosen as we demonstrated in recent years that it allows to secure the regular distribution of the surface organic groups throughout the pore channels of

these silica solids, exhibiting a 2D hexagonal arrangement of the porous network comparable of that observed in the well-known SBA-15 silica.^[42–46] Indeed, we have reported using the same protocol some hybrid silica materials containing TEMPO units and we demonstrated the regular distribution of such radicals using advanced NMR techniques (Surface Enhanced NMR using Dynamic Nuclear Polarization) and EPR.^[43] Here, the as-obtained thiol containing solids will be named SBA-PrSH^x, where x corresponds to the theoretical TEOS:(3-mercaptopropyl)triethoxysilane molar ratio (Scheme 1).

Three mesostructured materials, SBA-PrSH^x (x = 6, 10, 30), were fully characterized by N₂ adsorption-desorption at 77 K and elemental analyses (Si and S), and the results are summarized in Table 1.

We first chose a TEOS:(3-mercaptopropyl)triethoxysilane molar ratio of ca 30 because, in these conditions, thiol sites are isolated and very distant from each other (0.3 SH group per nm²), whereas for a ratio of 10, these sites remain regularly distributed but are closer to each other (0.9 SH group per nm²). Finally, we decided to prepare a thiol-containing silica support using a TEOS:thiol ratio of 6. With such a high loading of surface SH groups (theoretical SH density of ca 1.8 SH per nm²), the thiols distribution and isolation were no longer controlled and the porous network of the silica framework was not mesostructured anymore (see below). This solid was intentionally prepared to check the influence of site isolation/distribution on the catalytic performances.

As expected, surface area, pore volume and diameter of these materials increased when the TEOS:(3-mercaptopropyl)triethoxysilane molar ratio increased, and the most diluted samples, namely SBA-PrSH³⁰ and SBA-PrSH¹⁰ exhibited key physical features corresponding to SBA-15 type materials: large surface area from 930 to 970 m²/g, important pore volume from 0.8 to 1.4 cm³/g, calibrated large pore diameters from 5 to 8 nm (Table 1) and the expected 2D hexagonal arrangement of the pore channels as demonstrated by HR-TEM images and type IV N₂ adsorption/desorption isotherms (see ESI). At the opposite, the important amount of thiol precursor used to prepare SBA-PrSH⁶ materials prevented the efficient structuration of the porous network and the regular distribution of the SH groups as shown by TEM micrographs (see ESI) and the modification of the texture compared to SBA-PrSH³⁰ and SBA-PrSH¹⁰. Indeed, this material exhibits lower surface area (627 m²/g) and pore volume (0.4 cm³/g), along with a large distribution of small mesopores (from 2 to 7 nm with a mean diameter of ca 3 nm -



Scheme 1. Synthesis of the thiol containing mesoporous silica matrices.

Table 1. Texture and SH loading of the thiol-containing solids.							
Entry	Solids	S _{BET} [m ² /g]	V _p [cm ³ /g]	D _p [nm]	Si: SH ^[a]	SH [mmol/g]	SH [/nm ²]
1	SBA-PrSH ³⁰	970	1.4	8	28	0.5	0.3
2	SBA-PrSH ¹⁰	930	0.8	5	9	1.4	0.9
3	SBA-PrSH ⁶	627	0.4	3	6	1.9	1.8

[a] Si:S ratio according to elemental analysis.

see ESI, Figure S9). This lack of structuration was expected since functional silicas with low "Si:organic" molar ratio were often found disordered and this cut off ratio mainly depends on the size of the organic group.^[47]

Different loadings of Pd in the final materials - and thus the number of SH putatively coordinating the palladium centers - were targeted and obtained by varying the concentration of the solution containing Pd(OAc)₂. Substoichiometric SH:Pd molar ratios were chosen, from 6 to 65, depending on the type of SBA-PrSH^x supports. The experimental SH:Pd ratios were determined by elemental analyses of sulfur and palladium and were found quite similar to the targeted nominal values as presented thereafter in Table 2.

For SBA-PrSH³⁰ (Table 2, Entries 1–4), SH:Pd ratios of 6, 12, 50 and 65 were targeted, and the experimental SH:Pd ratios as determined by elemental analyses were 8, 12, 57 and 65 respectively. The good accordance between the expected and the experimental ratios highlights the efficiency of the metallation method. For sake of clarity, all the metallated materials will be quoted SBA-PrSH^x.Pd^y with x corresponding to the Si:S molar ratio and y to the targeted SH:Pd molar ratio. Similar SH:Pd ratios of 6 and 65 were targeted for SBA-PrSH¹⁰ and SBA-PrSH⁶ materials. The experimental SH:Pd ratios were found equal to 7 for both SBA-PrSH¹⁰.Pd⁶ and PrSH⁶.Pd⁶ (Table 2, Entries 5 and 7) and 67 and 50 for SBA-PrSH¹⁰.Pd⁶⁵ and SBA-PrSH⁶.Pd⁶⁵ respectively (Table 2, Entries 6 and 8).

After palladium coordination onto these supports, the samples were fully characterized using N₂ adsorption-desorption and HR-TEM microscopy. The results show that the texture and the structuration of the pore networks were not affected by the metallation step (HR-TEM pictures in ESI). Only a decrease in surface area of ca 100 to 200 m²/g (depending of the quantity of loaded Pd) was observed as expected (see ESI for the exact quantification). HR-TEM analyses (bright field and HAADF-STEM) and Pd quantification by EDX also allowed to get more insight into the distribution of Pd within the samples. Concerning the mesostructured samples possessing regularly distributed SH groups (SBA-PrSH¹⁰.Pd⁶, SBA-PrSH¹⁰.Pd⁶⁵ and SBA-PrSH³⁰.Pd⁶, SBA-PrSH³⁰.Pd¹², SBA-PrSH³⁰.Pd⁵⁰, SBA-PrSH³⁰.Pd⁶⁵), a homogeneous distribution of Pd was detected by EDX without the formation of Pd NPs according to HR-TEM (see Figure 1A and Figure 1B2 and ESI). This result suggests the presence of isolated Pd atoms or very small undetectable Pd clusters throughout the solids. At the opposite, for samples SBA-

PrSH⁶.Pd⁶ and SBA-PrSH⁶.Pd⁶⁵ in which the regular distribution of surface SH groups was not secured, small palladium nanoparticles were observed (see Figure 1C and ESI). HR-TEM analysis also highlighted the presence of Pd nanoparticles/aggregates outside the silica frameworks for the most concentrated samples (SH/Pd = 6) containing a high content of surface thiols (namely SBA-PrSH¹⁰.Pd⁶ and SBA-PrSH⁶.Pd⁶-Figure 1B1 and Figure 1C1). In these samples, the palladium content as given by elemental analysis is thus not representative of the amount of Pd coordinated to the thiol groups into the pores of the materials. Unfortunately, our attempts to quantify such Pd content by EDX were not successful, giving unrealistic Pd loadings (higher than those given by elemental analysis in some cases).

Overall, these data highlight the fact that the regular distribution of the SH groups along with the density of surface SH groups and the SH/Pd ratios are important parameters to secure the distribution of Pd into the silica matrices as single

Table 2. Pd loadings in the mesoporous silicas supports according to elemental analyses.

Entry	Targeted materials	SH:Pd from EA	Pd [μmol/g] from EA	Pd [wt%]
1	SBA-PrSH ³⁰ .Pd ⁶	8	63	0.67
2	SBA-PrSH ³⁰ .Pd ¹²	12	42	0.45
3	SBA-PrSH ³⁰ .Pd ⁵⁰	57	9	0.10
4	SBA-PrSH ³⁰ .Pd ⁶⁵	65	8	0.08
5	SBA-PrSH ¹⁰ .Pd ⁶	7	190	2.02
6	SBA-PrSH ¹⁰ .Pd ⁶⁵	67	21	0.22
7	SBA-PrSH ⁶ .Pd ⁶	7	266	2.83
8	SBA-PrSH ⁶ .Pd ⁶⁵	50	35	0.37

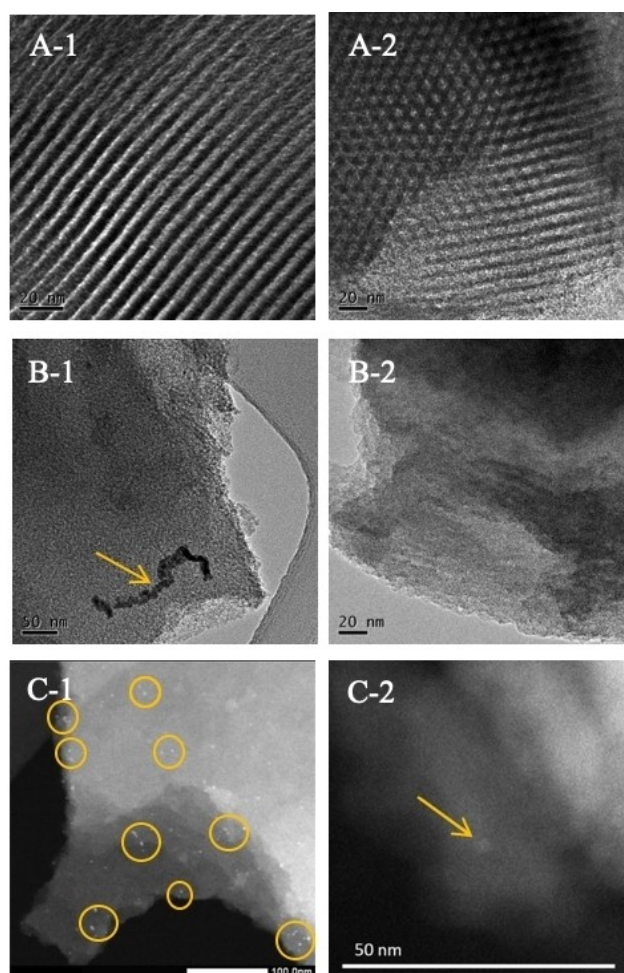
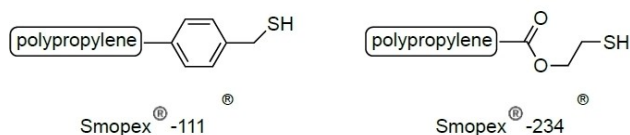


Figure 1. HRTEM micrographs of SBA-PrSH³⁰.Pd^y materials (A-1: y = 6 and A-2: y = 65) and SBA-PrSH¹⁰.Pd^y materials (B-1: y = 6 and B-2: y = 65). HAADF-STEM micrographs of SBA-PrSH⁶.Pd^y materials (C-1: y = 6 and C-2: y = 65). Palladium nanoparticles aggregate is indicated by a yellow arrow (B-1) and isolated palladium nanoparticles are highlighted by yellow circles (C-1).

atoms and not as Pd nanoparticles, in or outside the silica supports.

For sake of comparison, two commercially available thiol containing polymers, namely smopex[®]-234 and smopex[®]-111 (Scheme 2), known as Pd scavengers^[48] for coupling reactions, were used and metallated with palladium using the same protocol. Here again, high and low SH:Pd molar ratios were targeted and the resulting solids are quoted smopex[®]-234-Pd^x and smopex[®]-111-Pd^x (x = 6 or 50, see Table 3).



Scheme 2. Thiol functionalized polypropylene fibers: smopex[®]-111 and smopex[®]-234.

Entry	Samples	SH:Pd from EA	Pd [$\mu\text{mol/g}$] from EA	Pd [wt %]
1	smopex [®] -111-Pd ⁶	6	308	3.28
2	smopex [®] -111-Pd ⁵⁰	35	46	0.49
3	smopex [®] -234-Pd ⁶	8	242	2.58
4	smopex [®] -234-Pd ⁵⁰	45	49	0.53

[a] smopex[®]-111 and smopex[®]-234 contain 2.2 and 1.8 mmol/g of thiol groups respectively (Johnson Matthey specifications) and contain non-isolated SH groups.

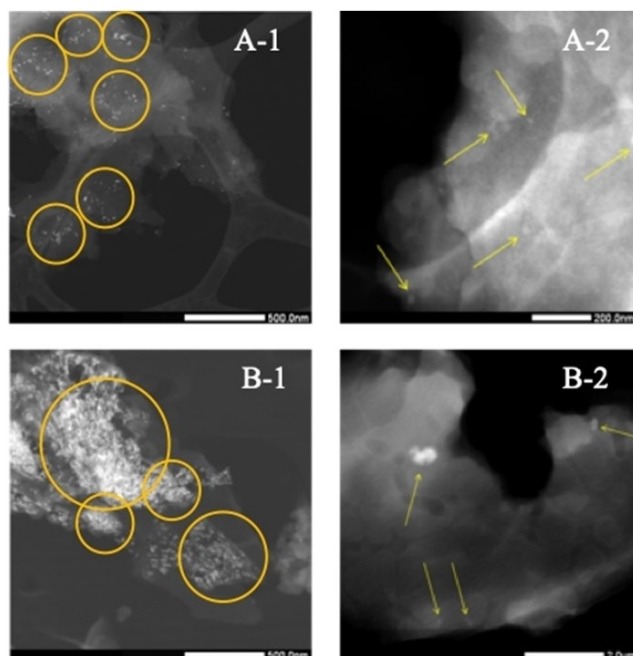


Figure 2. HAADF-STEM micrographs of smopex[®]-111-Pd^x materials (A-1: x = 6 and A-2: x = 50) and smopex[®]-234-Pd^x materials (B-1: x = 6 and B-2: x = 50). Palladium nanoparticles, and their aggregates, are highlighted by yellow circles (A-1 and B-1) and arrows (A-2 and B-2).

These materials were fully characterized by elemental analysis, N₂ adsorption/desorption and HR-TEM, before and after Pd incorporation. These polymers were found non-porous (surface area < 3 m²/g), with SH:Pd ratios determined by elemental analysis in the expected range (see Table 3).

Relatively large Pd nanoparticles/aggregates, exhibiting a broad size distribution, were detected in the most concentrated samples (SH:Pd = 6) for both types of smopex[®] whereas smaller Pd NPs were detected for the most diluted solids (see Figure 2).

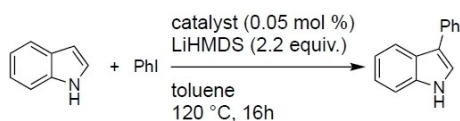
Overall, in all cases, the smopex[®] samples exhibited Pd NPs even at low Pd content (Table 3-entries 2 and 4) whereas the mesostructured samples containing similar Pd loadings did not exhibit Pd NPs (SBA-PrSH³⁰-Pd⁶ and SBA-PrSH³⁰-Pd¹²-Table 2 entries 1 and 2).

All the aforementioned solids were further used as catalysts for the selective arylation of free-indole. Quasi-stoichiometric amounts of indole (1 equiv.) and iodobenzene (1.2 equiv.) were used in the presence of 2.2 equiv. of lithium bis(trimethylsilyl)amide as the base and the catalyst loading was set to ca 0.05 mol% (Scheme 3). Finally, the reaction was conducted in toluene at 120 °C for 16 hours.

At the end of the reaction, the crude mixture was analyzed by gas chromatography to determine the conversion of indole and the yields in reaction products. ¹H NMR and ¹³C liquid state NMR were also used to confirm the molecular structure of all products. The catalytic results are presented in Table 4.

First, it is worth noting that the materials were all found more or less active in the targeted reaction with a complete selectivity towards the C-3 products as demonstrated by the good accordance between the conversion of indole, the yield in C-3 product and the high mass balance (see Table 4 columns 4, 5 and 7). These materials are thus the first examples of heterogeneous catalysts capable of performing the chemo- and regio-selective C-3 arylation of free indole. Table 4 also shows that the best materials for this reaction were the mesostructured materials containing the most isolated SH groups, namely SBA-PrSH³⁰-Pd^x (x = 6 to 65) with remarkable TONs for this reaction (calculated from the production of C-3 product) ranging from 608 to 1378. Only material SBA-PrSH¹⁰-Pd⁶ competed with SBA-PrSH³⁰-Pd⁶⁵, the less active catalyst from the SBA-PrSH³⁰-Pd^x series with a TON of 630. All the other materials which contain non-isolated and/or non-regularly distributed SH groups i.e. SBA-PrSH¹⁰-Pd⁶⁵, the SBA-PrSH⁶-Pd^x series and the smopex[®] samples were found far less active with TONs from 3 to 228. A closer look at the results from Table 4 also indicates a decrease in catalytic performances when the quantity of thiol groups inside the mesoporous materials increases for a given palladium loading as follows: SBA-PrSH³⁰-Pd⁶ (TON = 1380) > SBA-PrSH¹⁰-Pd⁶ (TON = 630) > SBA-PrSH⁶-Pd⁶ (TON = 98). All in one, these results clearly demonstrate the key role of the SH isolation and distribution in the silica matrices to yield highly active heterogeneous catalysts.

We could also observe, for each series, an increase of the catalytic performances with the loading of Pd. Indeed, for a given Si:S ratio, the higher the palladium content, the higher the TONs. For instance, we observed for SBA-PrSH³⁰-Pd^x (Table 3, entries 1–4) and SBA-PrSH¹⁰-Pd^x (Table 3, entries 5–6) that TONs



Scheme 3. Catalytic arylation of free indole with SBA-PrSH^x-Pd^y or smopex^x-Pd^x catalysts.

Table 4. Catalytic performances of the SBA-PrSH^x-Pd^y and smopex^x-Pd^x solids.

Entry	Materials	Pd ^[a]	Conv. [%]	Yield ^[b] [%]	TON ^[c]	Mass balance [%]
1	SBA-PrSH ³⁰ -Pd ⁶	0.046	65	63	1378	98
2	SBA-PrSH ³⁰ -Pd ¹²	0.035	51	50	1415	98
3	SBA-PrSH ³⁰ -Pd ⁵⁰	0.044	32	30	691	98
4	SBA-PrSH ³⁰ -Pd ⁶⁵	0.061	41	37	608	96
5	SBA-PrSH ¹⁰ -Pd ⁶	0.043	31	27	630	96
6	SBA-PrSH ¹⁰ -Pd ⁶⁵	0.034	10	6	151	96
7	SBA-PrSH ⁶ -Pd ⁶	0.034	15	3	98	89
8	SBA-PrSH ⁶ -Pd ⁶⁵	0.061	10	4	83	95
9	smopex ^x -111-Pd ⁶	0.043	15	11	228	97
10	smopex ^x -111-Pd ⁵⁰	0.053	14	9	180	95
11	smopex ^x -234-Pd ⁶	0.031	8	5	161	97
12	smopex ^x -234-Pd ⁵⁰	0.068	5	0	3	95

[a] The quantity of Pd in the catalytic tests is given in mol%. [b] Yield corresponds to the yield in C-3 arylated product. [c] TON is calculated from the yield of C-3 product (TON = yield/catalyst loading).

were multiplied by more than 2 and by almost 10 respectively, from the less palladium loaded material to the more palladium loaded material.

From the characterization of the catalysts by HR-TEM and the catalytic tests, it seems that Pd NPs are detrimental for catalysis, since the catalysts containing NPs are less productive than those without NPs. Accordingly, our current explanation is that the catalytic performances of the most active solids, that do not exhibit Pd NPs, are related to the presence of Pd(II) complexes yielded by the strong coordination of the thiolate ligands through the deprotonation of the thiol groups and the protonation of the acetate ligands, leading to the formation of acetic acid. This phenomenon was already reported when Pd(acetate)₂ and thiols, or substituted thioethers, in stoichiometric ratios, are allowed to react in solution, but also in cross linked Chitosan polymers containing mercaptopropylsilyl groups.^[49,50] However, the stability and the nuclearity of such Pd(II) complexes are difficult to assess since they depend on the acidity and the steric hindrance of the thiol ligands.^[49] In our case, we can hypothesize that such Pd(II) thiolate complexes are formed preferentially when the materials contain regularly distributed and isolated surface thiol groups. At the reverse, when the concentration of thiols increases and when the thiol isolation is not guaranteed, the growth of NPs is observed. The presence of such NPs is a bit surprising as it is generally reported when reducing agents (NaBH₄ for example) are used. However, it is worth noting that Pd NPs were also observed on Polyhedral oligomeric Silsesquioxane containing dodecanethiol groups coordinating Pd when the material was heated up to

120 °C.^[51] In our case, no thermal treatment was applied to the solids. Thus, the Pd NPs might be generated, when the concentration of thiols is high and the thiols isolation were not secured, during the drying of the solids under vacuum.

As productivity and selectivity of heterogeneous catalyst are not the only key parameters to discriminate the best catalytic systems, we thus also evaluated the Pd leaching during the catalytic reactions using hot filtration tests (also known as split tests) for the more productive catalysts (SBA-PrSH³⁰-Pd⁶). These tests were performed as follows: after 30 minutes of reaction at 120 °C (conversion of ca 5%), the catalyst was rapidly removed by filtration under argon and the collected filtrate was further stirred for an extra 15.5 h at 120 °C before analysis by GC-FID. The Pd content in the reaction products, after concentration of the reaction mixture to dryness, was also analyzed by ICP-MS analyses. The split tests results indicate that the material containing the highest loading of palladium (SBA-PrSH³⁰-Pd⁶) exhibited substantial leaching of highly active Pd species as the conversion in the liquid phase increases from 5% to 46% with a Pd content in the products of 1.7 ppm. At the opposite, the most diluted material, namely SBA-PrSH³⁰-Pd⁶⁵, was much more leaching resistant with a conversion in the liquid phase reaching only 11% and only 0.5 ppm of Pd was detected.

This split test confirms that it was possible to perform the arylation of indole with a solid catalyst (and not only with molecular complexes) with very little leaching and high TON allowing the production of almost pure arylated products. However, this result does not imply that the catalytic reaction occurs *via* a heterogeneous catalytic process.

The negligible Pd leaching for SBA-PrSH³⁰-Pd⁶⁵ prompted us to test the catalyst re-usability. To do so, a 1st catalytic test was performed using 0.051 mol% of Pd and stopped after 16 h of reaction. A conversion of 31% (i.e. far from full conversion) and a yield of 30% were reached which translate respectively into a TON of 608 and 598. The solid was further subjected to another catalytic run. After the exact same reaction time than that used for the first run, the catalyst was removed by filtration and the reaction mixture was quenched and analysed. Similar rate, selectivity and productivity were observed (conversion = 30% and TON = 600; yield = 29% and TON = 567), showing the re-usability of the catalyst.

Conclusion

In conclusion, we have developed here, for the first time, Pd-based heterogeneous catalysts for the selective C-3 arylation of free-indole. These materials were obtained using tailored made thiol-functionalized silica supports to anchor the palladium centers. It was shown that some of the solids exhibited remarkable catalytic performances in the targeted reaction, yielding exclusively the C-3 product with palladium loadings as low as 0.05 mol%. It was also demonstrated that the regular distribution and the isolation of surface thiol groups along with the amount of loaded Pd *per* SH group play a key role on the catalytic performances. The solids containing the most isolated surface SH groups (0.3 SH/nm²) were found the best catalysts.

From the series, the material exhibiting the highest loading of Pd (SH:Pd=6) was the most productive catalyst, reaching 70% of conversion and very high TON of ca 1400. However, leaching of active Pd species was detected (1.7 ppm). The best compromise was found for a specific solid containing isolated surface thiol groups (0.3 SH/nm²) and a low loading of Pd (SH/Pd=65). It exhibited a high TON (608) with a very low Pd leaching of 0.5 ppm according to split tests. This solid was also successfully re-used without any significant loss of catalytic activity/productivity/selectivity. These Pd-supported catalysts are thus very promising for the preparation of arylated indoles that are ubiquitous in active pharmaceutical ingredients.

Experimental Section

Synthesis of SBA-PrSH^x materials

Representative procedure for SBA-PrSH³⁰

A homogeneous solution of P123 (8.4 g), H₂O (333 mL) and HCl 37% (878 μ L) was added to a mixture of TEOS (20 mL, 90 mmol) and (3-mercaptopropyl)triethoxysilane (794 μ L, 3.0 mmol). The reaction mixture was stirred for 2 h at room temperature and then warmed up to 45 °C, at which temperature NaF (154 mg, 3.67 mmol) was added. The mixture was stirred at this temperature for 72 h. The resulting solid was filtered and washed with H₂O (100 mL), EtOH (100 mL) and acetone (100 mL). The surfactant was removed by Soxhlet extraction with EtOH during 48 h. The solid was further filtered, washed with acetone (100 mL) and MeOH (100 mL). It was then suspended in an aqueous solution of HCl 2 M (500 mL) and stirred at 45 °C for 2 h. After filtration, washings with H₂O (100 mL), EtOH (100 mL), acetone and Et₂O (100 mL) and drying at 135 °C under vacuum (10⁻⁵ mbar), 4.7 g of SBA-PrSH³⁰ was obtained as a white powder.

Materials SBA-PrSH¹⁰ and SBA-PrSH⁶ were prepared analogously by changing the TEOS:(3-mercaptopropyl)triethoxysilane ratio while keeping a constant Si:P123 molar ratio.

Incorporation of Pd in the SBA-PrSH^x materials

A mixture of SBA-PrSH^x material (250 mg), Pd(OAc)₂ (Z mg, depending on the targeted Pd loading) and THF (10 mL) was stirred under argon at room temperature for 4 h. The solid was filtered and washed thoroughly with THF (3 \times 10 mL), DCM (3 \times 10 mL) and Et₂O (2 \times 10 mL). The resulting solid was dried under vacuum (10⁻² mbar) overnight.

Catalytic tests

To a Schlenk tube equipped with a magnetic stirring bar were added indole (0.5 mmol), LiHMDS (1.1 mmol, 189 mg, 2.2 equiv.) and the catalyst (either SBA-PrSH^xPd^y materials, smopex[®]-111-Pd^x or smopex[®]-234-Pd^x, 0.25 μ mol of Pd, 0.05 mol% Pd) in a glove box. The flask was sealed with a silicon septum and transferred out of the glove box. Dry toluene (4 mL), iodobenzene (67 μ L, 0.6 mmol, 1.2 equiv.) and dodecane (150 mg as internal standard) were further added through the septum. The reaction was capped and stirred at 120 °C. After 16 h, the reaction mixture was quenched with 2 mL of methanol and stirred for 15 min. The organic phase was injected in the GC-FID for analysis.

Leaching tests – hot filtration/split tests

The reaction was conducted as detailed before at 120 °C during 30 min. After 30 min, the catalyst was rapidly removed by filtration under argon and the hot liquid phase was transferred to another Schlenk tube under argon and stirred for an extra 15.5 h at 120 °C. The reaction mixture was then quenched with 8 mL of MeOH and analyzed by GC-FID. The solution was finally concentrated to dryness and the Pd content was analysed by ICP-MS.

Recycling tests

The reaction was conducted as detailed before. After 16 h of reaction, the mixture was quenched with MeOH (4 mL). After 5 min at r.t., the reaction mixture was filtered, and the spent solid catalyst was further washed three times with 8 mL of MeOH. Then, the catalyst was recovered and resubmitted to catalysis.

Acknowledgements

This work has been carried out within the H-CCAT project that has received funding from the European Union's Horizon 2020 research and innovation program under grant agreement No 720996.

Conflict of Interest

The authors declare no conflict of interest.

Keywords: Arylation · C–H activation · Heterogeneous catalysis · Mesoporous functionalized silica · Palladium

- [1] R. Rohini, P. Muralidhar Reddy, K. Shanker, A. Hu, V. Ravinder, *Eur. J. Med. Chem.* **2010**, *45*, 1200–1205.
- [2] T. C. Leboho, J. P. Michael, W. A. L. van Otterlo, S. F. van Vuuren, C. B. de Koning, *Bioorg. Med. Chem. Lett.* **2009**, *19*, 4948–4951.
- [3] S. Suzen, N. Das-Evcimen, P. Varol, M. Sarikaya, *Med. Chem. Res.* **2007**, *16*, 112–118.
- [4] J. Malmgren, A. Nagendiran, C.-W. Tai, J.-E. Bäckvall, B. Olofsson, *Chem. Eur. J.* **2014**, *20*, 13531–13535.
- [5] Y. Huang, Z. Lin, R. Cao, *Chem. Eur. J.* **2011**, *17*, 12706–12712.
- [6] L. Djakovitch, V. Dufaud, R. Zaidi, *Adv. Synth. Catal.* **2006**, *348*, 715–724.
- [7] D. Das, Z. T. Bhutia, A. Chatterjee, M. Banerjee, *J. Org. Chem.* **2019**, *84*, 10764–10774.
- [8] X. Wang, D. V. Gribkov, D. Sames, *J. Org. Chem.* **2007**, *72*, 1476–1479.
- [9] L. Duan, R. Fu, B. Zhang, W. Shi, S. Chen, Y. Wan, *ACS Catal.* **2016**, *6*, 1062–1074.
- [10] H. Veisi, M. R. Poor Heravi, M. Hamelian, *Appl. Organomet. Chem.* **2015**, *29*, 334–337.
- [11] H. Veisi, N. Morakabati, *New J. Chem.* **2015**, *39*, 2901–2907.
- [12] L. Wang, W. Yi, C. Cai, *Chem. Commun.* **2011**, *47*, 806–808.
- [13] B. S. Lane, M. A. Brown, D. Sames, *J. Am. Chem. Soc.* **2005**, *127*, 8050–8057.
- [14] Z. Zhang, Z. Hu, Z. Yu, P. Lei, H. Chi, Y. Wang, R. He, *Tetrahedron Lett.* **2007**, *48*, 2415–2419.
- [15] F. Bellina, F. Benelli, R. Rossi, *J. Org. Chem.* **2008**, *73*, 5529–5535.
- [16] G. Cusati, L. Djakovitch, *Tetrahedron Lett.* **2008**, *49*, 2499–2502.
- [17] B. Join, T. Yamamoto, K. Itami, *Angew. Chem. Int. Ed.* **2009**, *48*, 3644–3647; *Angew. Chem.* **2009**, *121*, 3698–3701.
- [18] S. Perato, B. Large, Q. Lu, A. Gaucher, D. Prim, *ChemCatChem* **2017**, *9*, 389–392.
- [19] M. Yamaguchi, K. Suzuki, Y. Sato, K. Manabe, *Org. Lett.* **2017**, *19*, 5388–5391.

- [20] Y. Mohr, M. Renom-Carrasco, C. Demarcy, E. A. Quadrelli, C. Camp, F. M. Wisser, E. Clot, C. Thieuleux, J. Canivet, *ACS Catal.* **2020**, *10*, 2713–2719.
- [21] J. Chen, J. Wu, *Angew. Chem. Int. Ed.* **2017**, *56*, 3951–3955.
- [22] L. Ackermann, M. Dell'Acqua, S. Fenner, R. Vicente, R. Sandmann, *Org. Lett.* **2011**, *13*, 2358–2360.
- [23] L. Huang, T. P. Ang, Z. Wang, J. Tan, J. Chen, P. K. Wong, *Inorg. Chem.* **2011**, *50*, 2094–2111.
- [24] L. Mercier, T. J. Pinnavaia, *Adv. Mater.* **1997**, *9*, 500–503.
- [25] T. Kang, Y. Park, J. Yi, *Ind. Eng. Chem. Res.* **2004**, *43*, 1478–1484.
- [26] S. Bagheri, M. M. Amini, M. Behbahani, G. Rabiee, *Microchem. J.* **2019**, *145*, 460–469.
- [27] L. Chai, Q. Li, Y. Zhu, Z. Zhang, Q. Wang, Y. Wang, Z. Yang, *Bioresour. Technol.* **2010**, *101*, 6269–6272.
- [28] A. de Mello Ferreira Guimarães, V. S. T. Ciminelli, W. L. Vasconcelos, *Appl. Clay Sci.* **2009**, *42*, 410–414.
- [29] K. F. Lam, C. M. Fong, K. L. Yeung, G. McKay, *Chem. Eng. J.* **2008**, *145*, 185–195.
- [30] B. Fotoohi, L. Mercier, *Hydrometallurgy* **2015**, *156*, 28–39.
- [31] K. Shimizu, S. Koizumi, T. Hatamachi, H. Yoshida, S. Komai, T. Kodama, Y. Kitayama, *J. Catal.* **2004**, *228*, 141–151.
- [32] R. L. Oliveira, W. He, R. J. M. Klein Gebbink, K. P. de Jong, *Catal. Sci. Technol.* **2015**, *5*, 1919–1928.
- [33] J. M. Richardson, C. W. Jones, *J. Catal.* **2007**, *251*, 80–93.
- [34] C. M. Crudden, M. Sateesh, R. Lewis, *J. Am. Chem. Soc.* **2005**, *127*, 10045–10050.
- [35] M. A. Hanif, I. I. Ebraldize, J. H. Horton, *Appl. Surf. Sci.* **2013**, *280*, 836–844.
- [36] S. El Hankari, A. El Kadiib, A. Finiels, A. Bouhaouss, J. J. E. Moreau, C. M. Crudden, D. Brunel, P. Hesemann, *Chem. Eur. J.* **2011**, *17*, 8984–8994.
- [37] J. Niu, M. Liu, P. Wang, Y. Long, M. Xie, R. Li, J. Ma, *New J. Chem.* **2014**, *38*, 1471–1476.
- [38] S. Hossain, J. H. Park, M. K. Park, M. J. Jin, *J. Korean Chem. Soc.* **2013**, *57*, 411–415.
- [39] L. A. Aronica, A. M. Caporusso, G. Tuci, C. Evangelisti, M. Manzoli, M. Botavina, G. Martra, *Appl. Catal. A* **2014**, *480*, 1–9.
- [40] H. Hagiwara, T. Nakamura, T. Hoshi, T. Suzuki, *Green Chem.* **2011**, *13*, 1133–1137.
- [41] S. Hayashi, A. Takigami, T. Koizumi, *ChemPlusChem* **2016**, *81*, 930–934.
- [42] M. P. Conley, C. Copéret, C. Thieuleux, *ACS Catal.* **2014**, *4*, 1458–1469.
- [43] D. Gajan, M. Schwarzwälder, M. P. Conley, W. R. Grüning, A. J. Rossini, A. Zagdoun, M. Lelli, M. Yulikov, G. Jeschke, C. Sauvée, O. Ouari, P. Tordo, L. Veyre, A. Lesage, C. Thieuleux, L. Emsley, C. Copéret, *J. Am. Chem. Soc.* **2013**, *135*, 15459–15466.
- [44] M. H. Lim, A. Stein, *Chem. Mater.* **1999**, *11*, 3285–3295.
- [45] T. Yokoi, H. Yoshitake, T. Tatsumi, *J. Mater. Chem.* **2004**, *14*, 951–957.
- [46] R. Mouawia, A. Mehdi, C. Reyé, R. J. P. Corriu, *J. Mater. Chem.* **2008**, *18*, 4193–4203.
- [47] A. Mehdi, C. Reyé, R. Corriu, *Chem. Soc. Rev.* **2011**, *40*, 563–574.
- [48] P. Stephanie, K. Pasi, *Platinum Met. Rev.* **2010**, *54*, 69–70.
- [49] M. Basato, D. Tommasi, M. Zecca, *J. Organomet. Chem.* **1998**, *571*, 115–121.
- [50] C.-H. Lu, D. Lu, P. Jiang, J. Li, Y. Lang, *Catal. Lett.* **2017**, *147*, 2534–2541.
- [51] C.-H. Lu, F.-C. Chang, *ACS Catal.* **2011**, *1*, 481–488.

Manuscript received: November 30, 2020
Revised manuscript received: January 20, 2021
Accepted manuscript online: January 20, 2021